PHILOSOPHICAL TRANSACTIONS OF THE ROYAL SOCIETY A MATHEMATICAL, PHYSICAL & ENGINEERING SCIENCES

Novel Applications of Raman Microscopy [and Discussion]

D. J. Gardiner, M. Bowden, P. R. Graves and R. B. Thompson

Phil. Trans. R. Soc. Lond. A 1986 **320**, 295-306
doi: 10.1098/rsta.1986.0118

Phil. Trans. R. Soc. Lond. A **320**, 295–306 (1986)
Printed in Great Britain

Novel applications of Raman microscopy

By D. J. Gardiner,[1] M. Bowden[1] and P. R. Graves[2]

[1] *School of Chemical and Life Sciences, Newcastle upon Tyne Polytechnic, Newcastle upon Tyne NE1 8ST, U.K.*

[2] *Materials Development Division, Atomic Energy Research Establishment, Harwell, Oxfordshire OX11 0RA, U.K.*

Raman microscopy is rapidly becoming established as a valuable non-destructive method for examination and chemical analysis of microscopic samples. The technique uses microscope optics to focus laser light onto a sample and to collect the inelastic (Raman) scattered photons which result. This Raman scattered light provides a vibrational spectrum of the sample with a typical spatial resolution of around 2 μm. By using this technique, high-temperature corrosion films formed in sulphur and oxygen containing atmospheres on titanium, molybdenum, hafnium, tantalum, zirconium, chromium, iron and 20/50/Nb stainless steel, have been characterized. In addition, the nature of a corrosion-inhibition complex formed on copper has been determined *in situ* and the mode of interaction of the EP lubricant additive, mercaptobenzothiazole, has been investigated by using the SERS effect. Studies of optical fibres, semiconductor films and lubricant films in rolling elastohydrodynamic contacts further illuminate the wide applicability of this technique.

Introduction

Raman spectroscopy provides a method for obtaining the vibrational frequencies of a molecule and hence its characteristic vibrational (Raman) spectrum. The Raman effect requires illumination of the sample by high intensity (I_0), monochromatic radiation and a collection and monochromator system to analyse the energy of the scattered radiation. This scattered radiation will comprise elastically scattered Rayleigh photons of intensity around $10^{-5}\ I_0$ and inelastically scattered Raman photons of intensity around $10^{-8}\ I_0$. The Raman scattered photons may arise following the promotion of a vibrational transition in the sample and thus have a lower energy than the incident photons (Stokes–Raman scatter), or may abstract a vibrational quantum and thus be higher in energy than the incident photons (anti-Stokes–Raman scatter). The latter requires the sample molecules to be in a vibrationally excited state and thus is less probable than the former. The Stokes–Raman scatter is usually analysed, resulting in a Raman spectrum which gives scattering intensity as a function of Raman shift (frequency in reciprocal centimetres).

The development of Raman microscopy as a non-destructive microanalytical method, effectively started after a report (Rosasco 1975) from the National Bureau of Standards (NBS) in Washington presented at the fourth international conference on Raman spectroscopy in 1974. The NBS system comprised a microscope objective to focus the laser down to around 1 μm, standard Raman collection optics to focus the magnified image onto the monochromator entrance slit and a separate 180 ° opposed long working-distance objective with which to view the sample in white light. This system, although effective, has limitations in terms of ease of use, particularly with respect to sample mounting and alignment. At the same Raman

conference, Delhaye and co-workers (Delhaye & Dhamelincourt 1975) described a micro-Raman system based on a conventional white-light microscope. This system, in addition to allowing single-point analysis, created a monochromatic image of sample area and, by using a vidicon detector, the sample could be viewed in Raman light. This Raman imaging allows selective viewing of discrete sample components with a spatial resolution of the order of 1 μ.

Although Raman imaging has been further developed by the Lille group and involves the use of intensified diode-array detectors and improved spectrographic dispersion, the simpler single-point analysis microscopes have been more routinely used in a wide range of research fields. The construction of a simple microscope attachment for a Raman spectrometer is relatively straightforward as indicated by Cook & Loudon (1979). Several commercial systems are available, designed both for specific spectrometers and for attachment to any conventional Raman system.

The microscopes described here were designed in conjunction with B and G Spectroscopic Components Limited, for our research programme and have been used effectively with single channel, vidicon and diode array spectrometers.

Raman-microscope design

The essential function of the Raman-microscope attachment is to allow the sample to be exposed to either the focused laser or general white-light illumination and to allow light from the sample to be directed either to the monochromator or to a viewing system. For safe operation, a vidicon and monitor are most frequently used. The RMIII system used in this work follows the basic configuration described by Cook & Louden (1979) but incorporates more efficient laser input optics and an interchangeable beamsplitter.

The arrangement of the RMIII and related Raman equipment is illustrated in figure 1. Lens *a* spreads the laser light both to give a virtual source at the correct image plane and to fill the objective. The objective serves to focus the laser light to a point and to collect the Raman-scattered radiation. The scattered light is brought to an intermediate focus before lens *b* matches it to the aperture of the monochromator. A white-light epi-illuminator can be swung into position to allow the sample to be viewed by a vidicon camera with the prism removed. The position of the focused laser spot can be determined by the camera, with the ND filter used for protection, and registered by an electronic marker in the video system. Some key aspects of the performance of such a system are the efficiency in the use of the available laser power and in collecting the scattered radiation, the spatial resolution in the sample and, to a lesser extent, the feasibility of making polarization measurements.

The optical configuration is designed to make the most efficient use of the laser radiation entering the microscope. The measured losses in lenses *a* and *b* and the prism are less than 1% and losses in the objective vary between 5 and 10% on each pass, according to the particular lens used. The dielectric beamsplitters have nearly constant values of reflectivity, R, and transmissivity, T, throughout the spectral region of interest and the efficiency is determined primarily by the product RT. A choice of 50% for R and T gives the highest value of 25% for the product. A considerable reduction in the power density at the sample for photosensitive materials, can be achieved at the expense of only a relatively small reduction in RT by the selection of a suitable beam splitter.

Spatial resolution in Raman spectroscopy is not easily defined. The size of the focused spot

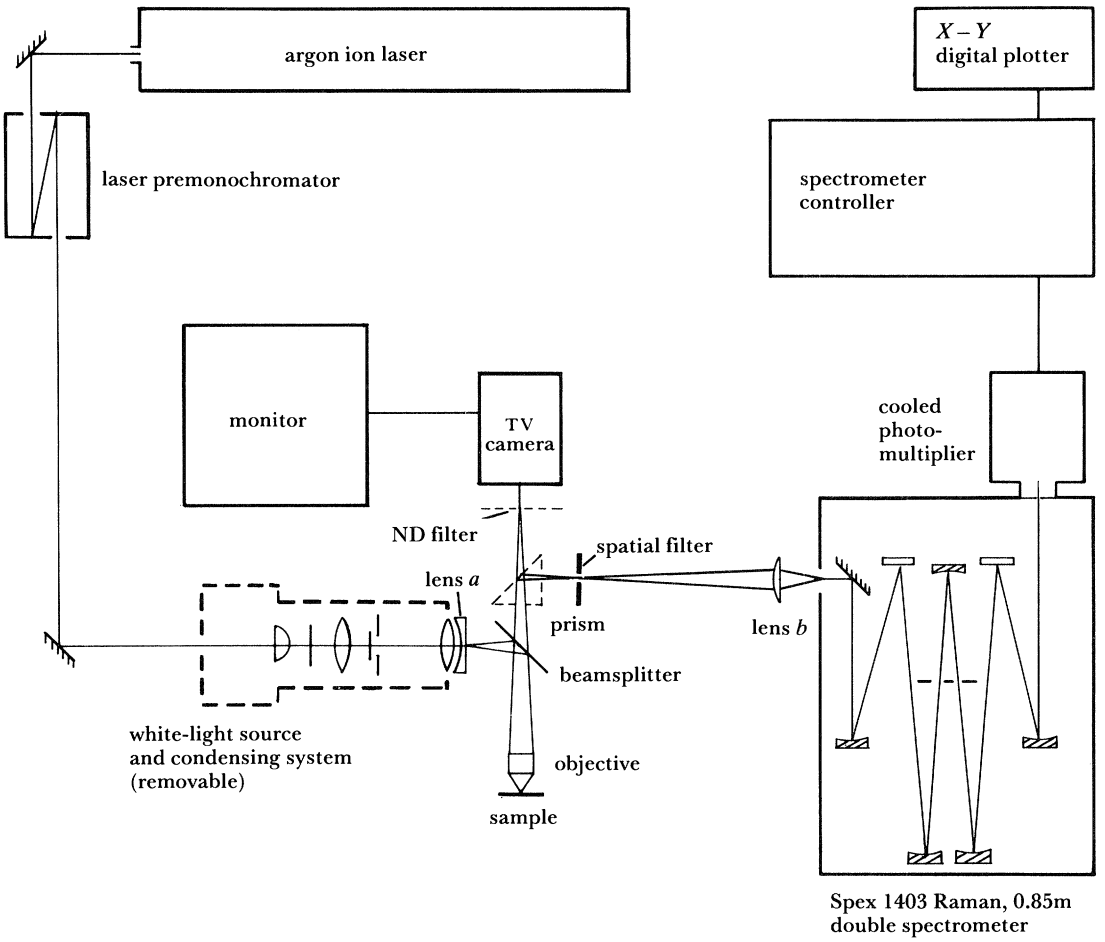

FIGURE 1. Schematic layout of the single-channel Raman-microscope system.

is measurable and is in the region of 2 μm for the most frequently used objective of ×40 magnification. Unless the sample under investigation is of very good optical quality, however, the detected Raman scatter will be from a much larger region than 2 μm because of spreading of the laser excitation by the microstructure of the sample. If high spatial resolution is important, a spatial filter can be incorporated in the image plane at the intermediate focus (see figure 1). This improved resolution normally results in a weaker Raman signal and is therefore used only when necessary. Filtering at this point in the system can also be used to reduce fluorescent backgrounds.

Experiments to determine spatial resolution are summarized in figures 2 and 3. Edge-response measurements with a highly reflecting surface with a sharply defined edge in place of the sample, were undertaken. The reflected laser light was measured in the approximate position of the matching lens *b*, thus simulating an idealized Raman experiment on an opaque sample, in which no spreading of the exciting radiation takes place. Edge responses for various objectives with and without a 100 μm diameter spatial filter are illustrated in figure 2 and the 95–5% cut-off edge values are listed in the table 1.

Edge response in an actual Raman experiment is illustrated in figure 3. A 1 μm thick CdS film on a glass substrate was fragmented by the thermal shock of a laser pulse to produce an

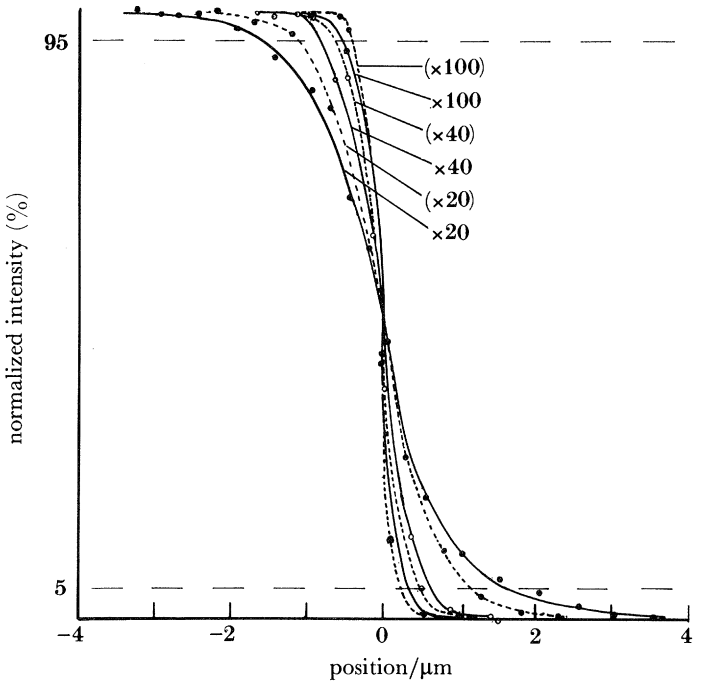

FIGURE 2. Edge-response plots for a highly reflective surface for objectives of different magnification with (denoted by figures in parenthesis) and without 100 μm spatial filter.

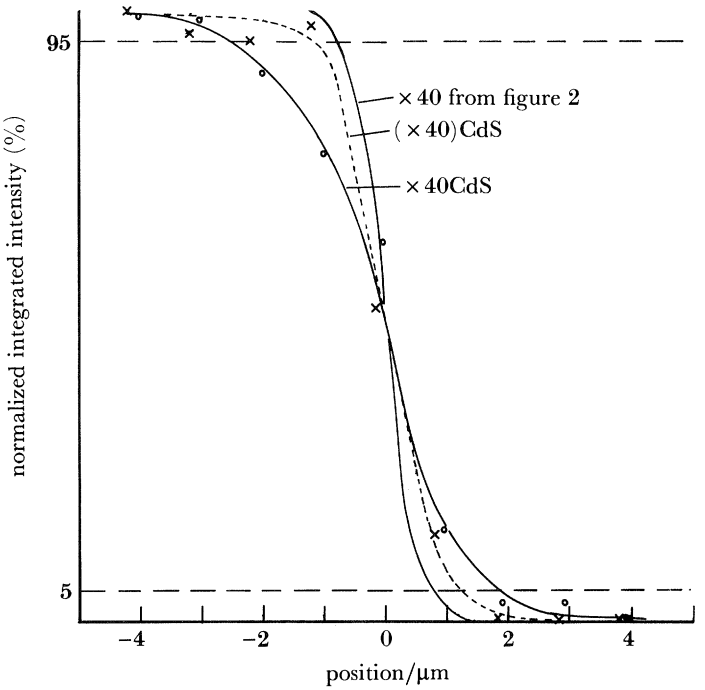

FIGURE 3. Raman edge-response plots from 1 μm CdS film, for × 40 objective with (denoted by figures in parenthesis) and without 100 μm spatial filter.

PHILOSOPHICAL TRANSACTIONS OF THE ROYAL SOCIETY A MATHEMATICAL, PHYSICAL & ENGINEERING SCIENCES

Table. 1. Spatial resolution data

objective	×20	×40	×100
numerical aperture	0.40	0.65	0.90
cut-off/μm	3.5	1.6 (4.6)	0.9
cut-off with spatial filter/μm	2.9	1.2 (2.1)	0.6

edge. The integrated intensity of the 297 cm^{-1} band of CdS was measured at intervals of 1 μm across the film edge. The importance of spatial filtering is clearly demonstrated and the cut-off values are listed in parentheses in the table 1. The corresponding curve from figure 2 is included for comparison.

Measurements of polarization ratios are relatively difficult to interpret in Raman-microscope experiments. Not only does the beamsplitter alter the state of polarization of the scattered radiation, but the polarization of the exciting-laser radiation in the sample volume is complicated by having been focused by a high numerical-aperture lens. The interpretation of such experiments has been discussed in detail by Turrell (1984). Useful measurements are shown to be possible but the need to use a scrambler involves some experimental difficulty in Raman microscopy because the beam of scattered radiation does not have a large enough diameter for a scrambler to function effectively. We have measured depolarization ratios by including the scrambler inside the monochromator.

The results reported in this paper were obtained using either a Spex 1403 0.85 m scanning double monochromator as depicted in figure 1 or a Spex Triplemate with a 512 element photodiode array.

Corrosion film characterization

Corrosion products of the pure metals, molybdenum, hafnium, titanium, tantalum and zirconium, have been investigated in atmospheres of high sulphur and low oxygen potential at elevated temperatures. These metals are potential minor constituents of alloys for use in these environments. It is suggested that such alloys will resist sulphidation by preferentially forming the sulphide of one of the minor components to form a compact barrier layer. We have obtained spectra from reference materials of possible corrosion products and compared them with spectra from corroded surfaces of the pure metals.

The spectra collected together in figures 4 and 5, reveal that in the cases of titanium, tantalum and zirconium it is, respectively, both the anatase and rutile modifications of TiO_2, β-Ta_2O_5, and monoclinic ZrO_2 which are formed. Molybdenum clearly produces MoS_2 and, in the case of hafnium, where a cross section of the sample was examined, regions of both HfO_2 and HfS_2 were found.

The production of corrosion resistant oxide coatings with good mechanical properties is an important aim of the research done at the Atomic Energy Research Establishment, to support the advanced gas-cooled reactor programme. The reactor fuel is contained within ribbed stainless steel tubes (fuel cans) made from nickel–chrome stainless steel containing a small amount of niobium (20Ni–25Cr–Nb). Preoxidation of such cans, followed by oxidation cycling leads to the formation of a layer of metal oxide that is 20–40 μm thick. X-ray diffraction and

PHILOSOPHICAL TRANSACTIONS OF THE ROYAL SOCIETY A MATHEMATICAL, PHYSICAL & ENGINEERING SCIENCES

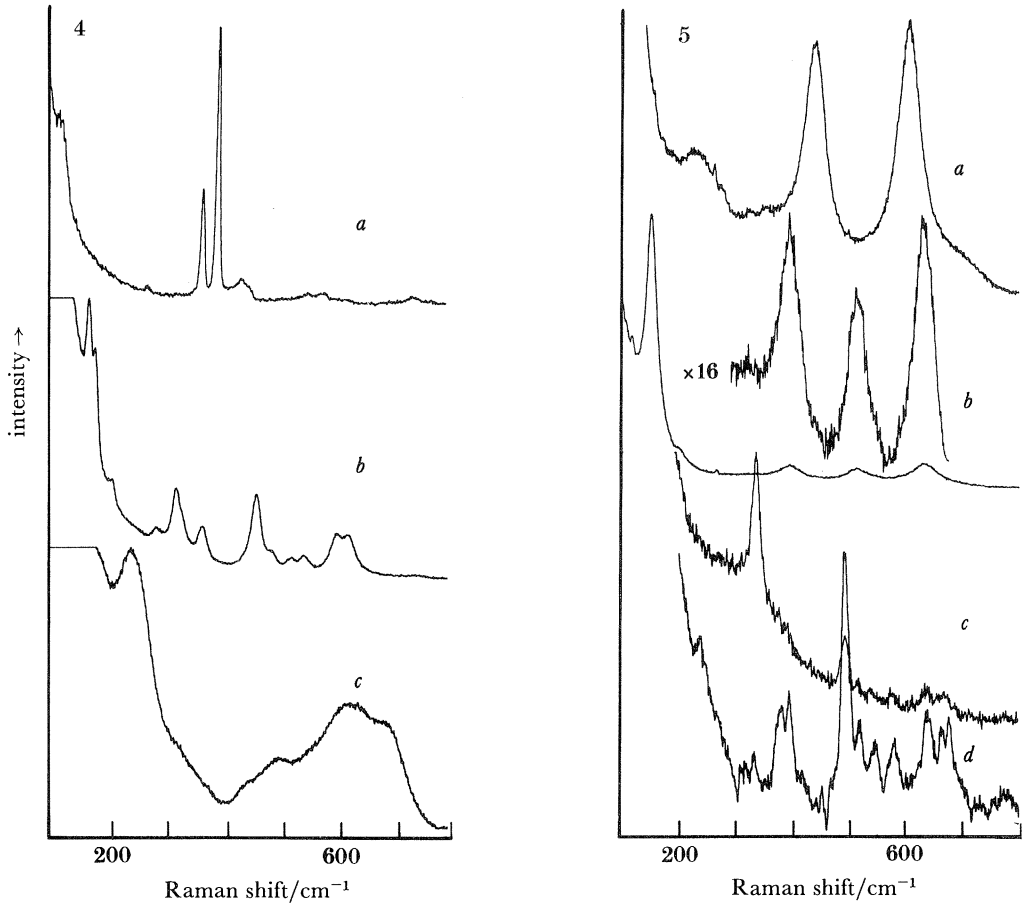

FIGURE 4. Raman spectra of (*a*) molybdenum disulphide, (*b*) zirconium dioxide and (*c*) tantalum pentoxide obtained from the surfaces of the pure metals following exposure to high sulphur and low oxygen potential atmospheres at temperatures of less than 750 °C.

FIGURE 5. Raman spectra which show duplex corrosion scale formation: (*a*) rutile and (*b*) anatase titanium dioxide spectra obtained from different regions of the same sample of pure titanium and (*c*) the surface and (*d*) interior of a corrosion scale formed on hafnium, showing a band due to hafnium disulphide at 338 cm^{-1} and bands due to the dioxide on the surface and hafnium dioxide only from the interior.

conventional Raman spectroscopy show the oxide scale to the composed of a number of different oxide phases.

However, neither technique can show the distribution of the phases throughout the oxide scale. By using the multichannel Raman microscope system it has been possible to scan a transverse section of a small piece of oxidized fuel can and obtain a Raman composition profile of the oxide scale. Figure 6*a* shows the Raman spectral profile recorded at 4 μm intervals through the scale. The results identify both phases of the duplex scale structure. An underlying layer of chromium oxide is progressively replaced by the outer layer of manganese chrome spinel ($MnCr_2O_4$) which verifies the elemental analysis obtained from elastic recoil analysis (ERDA) and Auger electron spectroscopy (AES).

In figure 6*b* the effect of a trace addition of cerium to the stainless steel is shown. Again after preoxidation, a protective oxide scale is formed but this time oxidative cycling produces a scale

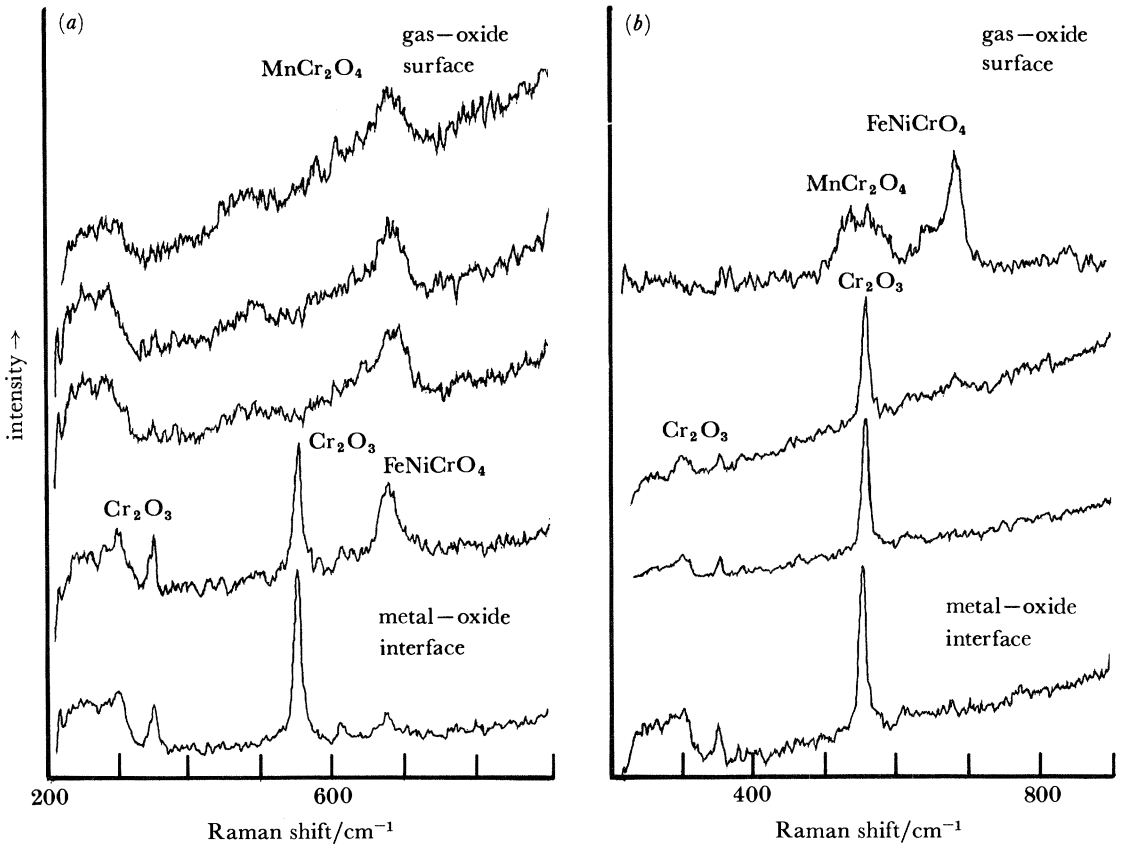

FIGURE 6. Raman spectra recorded at 4 μm step intervals through (*a*) the oxide scale on a 20/25/Nb steel sample and (*b*) 20/25/Nb steel containing cerium, showing the chemical composition at each point. The samples were oxidized in reactor stimulant gas for 306 h.

which is much thinner. Only the outer 1–2 μm is composed of $MnCr_2O_4$–$(FeNiCr)O_4$ spinel. The two profiles demonstrate the effect of cerium on scale formation and the passivating behaviour of the protective chromium oxide layer.

The Raman microscope thus enables chemical analysis of oxide scales with 2 μm resolution, which has previously not been possible with any other technique. *In situ* Raman measurements of oxide growth, which are currently being carried out, are expected to provide a much greater insight into the mechanism by which oxide scales develop.

LUBRICANT ADDITIVES

Raman microscopy offers the opportunity to study corrosion or corrosion-inhibition processes *in situ*. This is best facilitated by using a long working distance objective. In this way the corrosion inhibition films formed on copper in acidic aqueous environments by alkyl substituted imidazoline-2-thione have been characterized by comparison of the Raman spectra from the copper surface to those obtained from copper complexes of the inhibitors prepared from simple copper salts (Gardiner *et al.* 1986).

Surface-enhanced Raman scattering (SERS) enables monolayers to be detected, in some

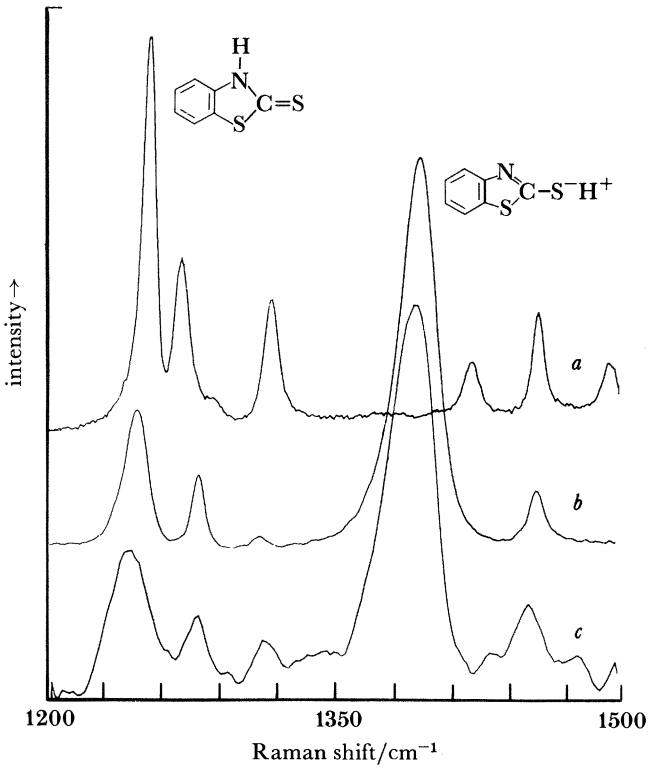

FIGURE 7. Raman spectra of (*a*) the solid, (*b*) a basic solution and (*c*) the SERS spectrum of surface adsorbed mercaptobenzothiazole.

instances, on specially prepared silver surfaces (Furtak & Reyes 1980). We have used this technique to study the mode of adsorption of the extreme pressure (EP) additive mercaptobenzothiazole on the surface of silver-plated stainless steel. Suetaka (Ohsawa *et al.* 1981) has studied the SERS spectrum of this molecule in an aqueous environment and has shown that it is the ionized form which is adsorbed onto silver electrode surfaces. Here we are concerned with the mode of adsorption from a typial non-polar lubricant medium. Figure 7 shows spectra of the solid (neutral form), of a basic solution (ionized form) and the SERS spectrum, from the surface of silver plated steel under a very dilute solution of the additive in hexadecane. In this non-polar environment, the Raman spectrum shows that it is again the ionized form which is adsorbed to the metal surface and is responsible for the molecule's EP properties.

ROLLING ELASTOHYDRODYNAMIC CONTACTS

In high-load bearing contacts, the bearing surfaces elastically deform around a thin film of the lubricant. These elastohydrodynamic contacts can be modelled by using a rolling steel ball on a glass plate which allows optical microscopic analysis of the contact region (Foord *et al.* 1970). Extension of this approach to Raman microscopy, allows a Raman spectrum of the lubricant in the contact to be obtained and monitored as a function of load, speed, and position within the contact.

The rig shown in figure 8 has been used to study the model lubricant 5P4E (a polyphenyl

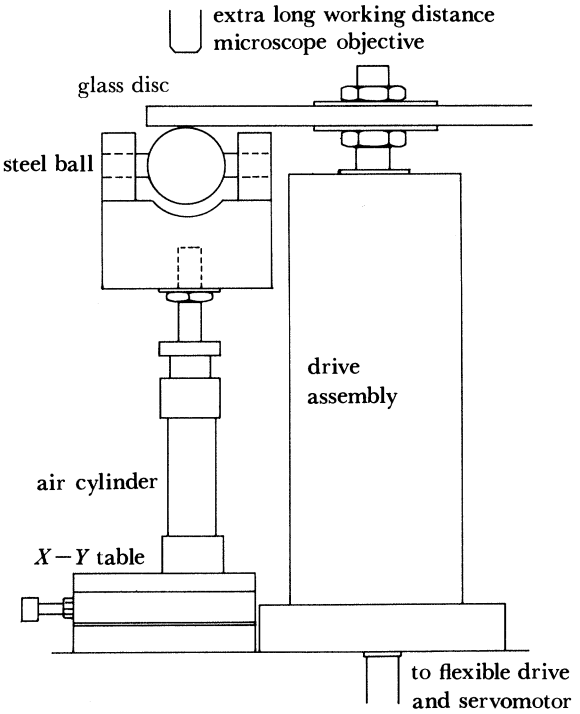

FIGURE 8. Dynamic ball and plate Raman lubrication rig.

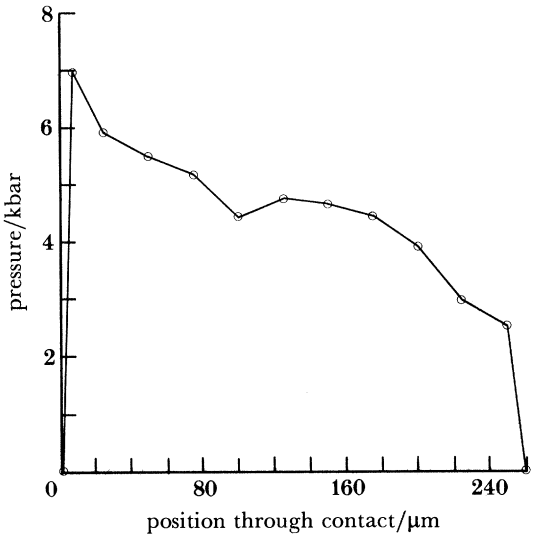

FIGURE 9. Pressure profile through a rolling EHD contact, determined from Raman shift measurements (260 μm represents entrance, 0 μm represents exit). (1 bar = 10^5 Pa).

ether). Our earlier work on stationary contacts, combined with the development of techniques for obtaining spectra from high-pressure diamond anvil cells under the microscope (Gardiner *et al.* 1983, 1984) allowed the calibration of the frequency of the strong ring breathing vibration of 5P4E as a function of pressure to be determined. In this way the pressure experienced by the lubricant in the contact could be monitored. The pressure profile obtained from the contact

rolling at a speed of 0.2 m s^{-1} with an applied load of 3.6 kg in the line of motion is shown in figure 9. This result is in good agreement with theory and confirms the presence of the Petrusevich pressure spike at the contact exit (Petrusevich 1951). Data obtained across the contact reveal a fairly flat pressure profile.

Optical fibres

A problem which has recently attracted interest is the degradation of optical communications fibres during use, due to the ingress of hydrogen (Mochizuki 1984). Hydrogen can be produced by the interaction between water and metals incorporated in the optical cable. It then permeates the fibre resulting in the attenuation of signals, particularly those transmitted at the important 1.3 or 1.55 μm wavelengths. The signal radiation may deteriorate either by absorption due to interstitial molecular hydrogen polarized by weak interaction with silica, or due to GeOH, SiOH or POH groups produced at elevated temperatures in a complex process in which, for example, the phosphorus centres can facilitate the formation of hydrogen atoms. The radial distribution, as the proportions of the different dopants vary, of hydrogen in its various forms would therefore provide a valuable insight into the processes involved. Experimental work on this problem has generally involved the use of infrared absorption spectroscopy, although Raman spectroscopy has demonstrated a significant presence of Si–H groups in lengths of hydrogenated fibres (Bibby & Ross 1984).

The technique of Raman microscopy has recently been applied to the study of radial distributions in optical fibres. Carvalho & Dumas (1984) report measurements of dopant profiles and radiation induced damage both in optical fibres and preforms. We have used Raman microscopy to investigate the radial distribution of dopants and Si–H bonds throughout

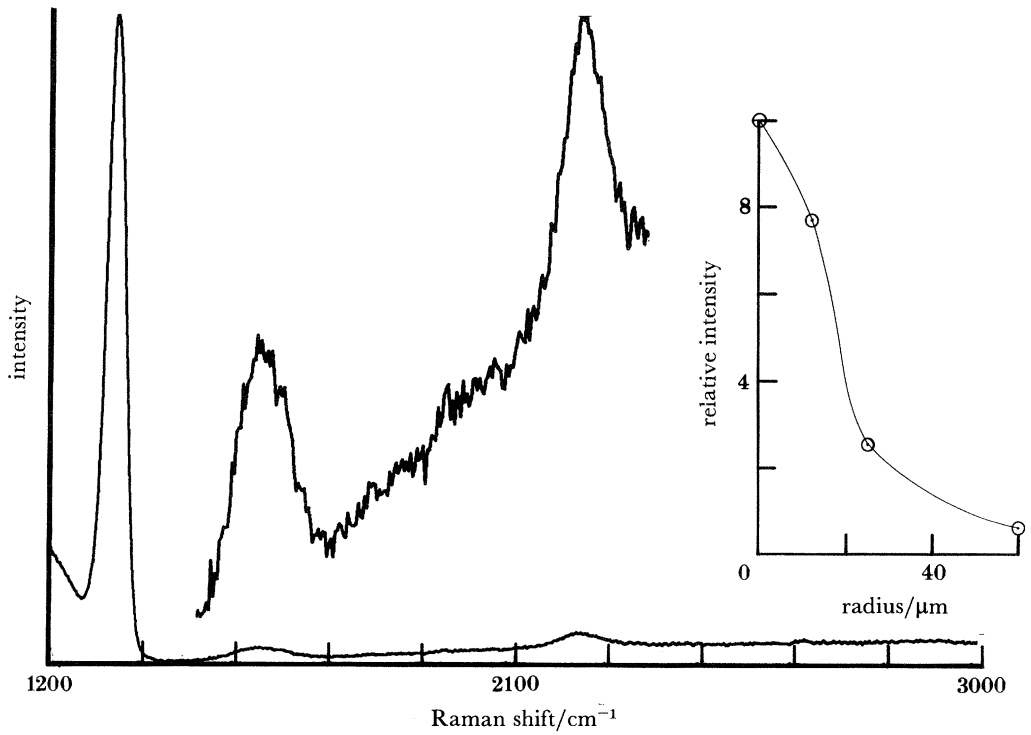

Figure 10. Optical fibre P_2O_5 dopant profile determined from Raman intensity data of the 1350 cm^{-1} band.

the core and cladding of graded index fibres which have been exposed to a hydrogen atmosphere at high temperature. As an example of the data obtainable, the spectrum shown in figure 10 was recorded from a region approximately 2 μm in diameter at the core centre of a fibre. The intense band at 1350 cm^{-1} arises from P–O vibrations of P_2O_5 and that band at 2240 cm^{-1} is due to Si–H vibrations. The inset is a plot of P–O band intensity as a function of distance from the core centre and thus reflects the concentration distribution of P_2O_5 and consequently the refractive index profile.

Conclusions

This paper has attempted to demonstrate the wide applicability of the Raman-microscope technique for non-destructive microanalysis. Of necessity, only a limited range of applications have been covered, other major areas of research involve problems in polymer science, micromineralogy, ceramics, semiconductor technology, biological and biochemical systems and forensic science. The number of papers describing research involving Raman microscopy is increasing and once diode array detectors become more cheaply available, the prospect for the development of instruments for Raman mapping of surfaces by using programmed stepper motor driven stages becomes brighter. It is clear that this relatively new technique is rapidly proving its value among the range of other microanalytical tools available to analytical scientists.

References

Bibby, G. W. & Ross, J. N. 1984 *Electron. Lett.* **20**, 182.
Carvalho, W. & Dumas, P. 1984 *J. Phys. Colloq.* **45**, 765.
Cook, B. W. & Louden, J. D. 1979 *J. Raman Spectrosc.* **8**, 249.
Delhaye, M. & Dhamelincourt, P. 1975 *J. Raman Spectrosc.* **3**, 33.
Foord, C. A., Wedeven, L. D., Westlake, F. J. & Cameron, A. 1970 Proc. Instn. mech. Engrs. **184**, 487.
Furtak, T. F. & Reyes, J. 1980 *Surf. Sci.* **93**, 351.
Gardiner, D. J., Baird, E., Gorvin, A. C., Marshall, W. E. & Dare-Edwards, M. P. 1983 Wear **91**, 111.
Gardiner, D. J., Bowden, M., Daymond, J., Gorvin, A. C. & Dare-Edwards, M. P 1984 *Appl. Spectrosc.* **38**, 282.
Gardiner, D. J., Gorvin, A. C., Gutteridge, C. & Raper, E. S. 1986 *Corros. Sci.* (In the press.)
Mochizuki, K., Namihira, K., Kuwazura, M. & Iwamoto, Y. 1984 *IEEE J. Quantum Electron.* **20**, 694.
Ohsawa, M., Matsuda, H. & Suetaka, W. 1981 *Chem. Phys. Lett.* **84**, 163.
Petrusevich, A. I. 1951 *Ezv.Akad. Nauk SSSR* **2**, 209.
Rosasco, G. J., Etz, E. S. & Cassatt, W. A. 1975 *Appl. Spectrosc.* **29**, 396.
Turrell, G. 1984 *J. Raman Spectrosc.* **15**, 103.

Discussion

R. B. Thompson (*Ames Laboratory, Iowa State University, Ames, Iowa, U.S.A.*). When an oxide grows on stainless steel, there will often be many different chemical compounds present at the same time. Can the Raman effect quantity the amounts of each which are present?

P. R. Graves. In our work at Harwell we have been able to locate discrete regions of particular phases (for example Cr_2O_3 and Fe_3O_4) distributed within scales. Provided that the laser exciting frequency is not close to an electronic absorption maximum, the Raman effect should be linear. Therefore it is possible to quantify the amounts of each chemical phase present in the scale if well characterized standards exist. The probe depth of the Raman microprobe is

always less than 2 μm, therefore, if the oxide scale is thick, it is necessary to mechanically or ion-beam thin. If the film is thin, quantitative thickness measurements are possible (see England *et al.* 1984).

To summarize: quantitative measurements can be made of oxide films on more ideal substrates and there is no reason why, in principle, such measurements could not be extended to more complex oxide scales.

Reference

England, W. A., Jenny, S. N., Greenhalgh, D. A. 1984 *J. Raman Spectrosc.* **15** (3), 156–159.

PHILOSOPHICAL TRANSACTIONS OF THE ROYAL SOCIETY A MATHEMATICAL, PHYSICAL & ENGINEERING SCIENCES